The "Millipede"—Nanotechnology Entering Data Storage

P. Vettiger, *Fellow, IEEE*, G. Cross, M. Despont, U. Drechsler, U. Dürig, B. Gotsmann, W. Häberle, M. A. Lantz, H. E. Rothuizen, R. Stutz, and G. K. Binnig

***Abstract*—We present a new scanning-probe-based data-storage concept called the "millipede" that combines ultrahigh density, terabit capacity, small form factor, and high data rate. Ultrahigh storage density has been demonstrated by a new thermomechanical local-probe technique to store, read back, and erase data in very thin polymer films. With this new technique, nanometer-sized bit indentations and pitch sizes have been made by a single cantilever/tip into thin polymer layers, resulting in a data storage densities of up to 1 Tb/in^2. High data rates are achieved by parallel operation of large two-dimensional (2-D) atomic force microscope (AFM) arrays that have been batch-fabricated by silicon surface-micromachining techniques. The very large-scale integration (VLSI) of micro/nanomechanical devices (cantilevers/tips) on a single chip leads to the largest and densest 2-D array of 32 $\times$ 32 (1024) AFM cantilevers with integrated write/read/erase storage functionality ever built. Time-multiplexed electronics control the functional storage cycles for parallel operation of the millipede array chip. Initial areal densities of 100–200 Gb/in^2 have been achieved with the 32 $\times$ 32 array chip, which has potential for further improvements. A complete prototype system demonstrating the basic millipede functions has been built, and an integrated five-axis scanner device used in this prototype is described in detail. For millipede storage applications the polymer medium plays a crucial role. Based on a systematic study of different polymers with varying glass-transition temperatures, the underlying physical mechanism of bit writing has been identified, allowing the correlation of polymer properties with millipede-relevant parameters. In addition, a novel erase mechanism has been established that exploits the metastable nature of written bits.**

***Index Terms*—Atomic force microscope (AFM) array chips, microscanner, millipede, nano-indentation, polymer films, scanning probe data storage, thermomechanical write/read/erase.**

I. Introduction

In THE 21st century, the nanometer will very likely play a role similar to the one played by the micrometer in the 20th century. The nanometer scale will presumably pervade the field of data storage. In magnetic storage today, there is no clear-cut way to achieve the nanometer scale in all three dimensions. The basis for storage in the 21st century might still be magnetism. Within a few years, however, magnetic storage technology will arrive at a stage of its exciting and successful evolution at which fundamental changes are likely to occur when current storage technology hits the well-known superparamagnetic limit. Several ideas have been proposed on how to overcome this limit. One such proposal involves the use of patterned magnetic media, for which the ideal write/read concept still needs to be demonstrated but the biggest challenge remains the patterning of the magnetic disk in a cost-effective way. Other proposals call for totally different media and techniques such as local probes or holographic methods. In general, if an existing technology reaches its limits in the course of its evolution and new alternatives are emerging in parallel, two things usually happen: First, the existing and well-established technology will be explored further and everything possible done to push its limits to take maximum advantage of the considerable investments made. Then, when the possibilities for improvements have been exhausted, the technology may still survive for certain niche applications, but the emerging technology will take over, opening up new perspectives and new directions.

Consider, for example, the vacuum electronic tube, which was replaced by the transistor. The tube still exists for a very few applications, whereas the transistor evolved into today's microelectronics with very large-scale integration (VLSI) of microprocessors and memories. Optical lithography may become another example: Although still the predominant technology, it will soon reach its fundamental limits and be replaced by a technology yet unknown. Today we are witnessing in many fields the transition from structures of the micrometer scale to those of the nanometer scale, a dimension at which nature has long been building the finest devices with a high degree of local functionality. Many of the techniques we use today are not suitable for the coming nanometer age; some will require minor or major modifications, and others will be partially or entirely replaced. It is certainly difficult to predict which techniques will fall into which category. For key areas in information-technology hardware, it is not yet obvious which technology and materials will be used for nanoelectronics and data storage.

In any case, an emerging technology being considered as a serious candidate to replace an existing but limited technology must offer long-term perspectives. For instance, the silicon microelectronics and storage industries are huge and require correspondingly enormous investments, which makes them long-term oriented by nature. The consequence for storage is that any new technique with better areal storage density than today's magnetic recording [1] should have long-term potential for further scaling, desirably down to the nanometer or even atomic scale.

The only available tool known today that is simple and yet provides these very long-term perspectives is a nanometer-sharp tip. Such tips are now being used in every atomic force microscope (AFM) and scanning tunneling microscope (STM) for imaging and structuring down to the atomic scale. The simple

Manuscript received January 25, 2002; revised February 14, 2002.

The authors are with IBM Research, Zurich Research Laboratory, 8803 Rüschlikon, Switzerland (e-mail: pv@zurich.ibm.com).

Publisher Item Identifier S 1536-125X(02)04585-4.

tip is a very reliable tool that concentrates on one functionality: the ultimate local confinement of interaction.

In the early 1990s, Mamin and Rugar at the IBM Almaden Research Center pioneered the possibility of using an AFM tip for readback and writing of topographic features for the purposes of data storage. In one scheme developed by them [2], reading and writing were demonstrated with a single AFM tip in contact with a rotating polycarbonate substrate. The writing was done thermomechanically via heating of the tip. In this way, storage densities of up to 30 Gb/in^2 were achieved, representing a significant advance compared to the densities of that day. Later refinements included increasing readback speeds up to a data rate of 10 Mb/s [3], and implementation of track servoing [4].

In making use of single tips in AFM or STM operation for storage, one has to deal with their fundamental limits for high data rates. At present, the mechanical resonant frequencies of the AFM cantilevers limit the data rates of a single cantilever to a few Mb/s for AFM data storage [5] and [6], and the feedback speed and low tunneling currents limit STM-based storage approaches to even lower data rates.

Currently, a single AFM operates at best on the microsecond time scale. Conventional magnetic storage, however, operates at best on the nanosecond time scale, making it clear that AFM data rates have to be improved by at least three orders of magnitudes to be competitive with current and future magnetic recording.

The objectives of our research activities within the Micro- and Nanomechanics project at the IBM Zurich Research Laboratory are to explore highly parallel AFM data storage with areal storage densities far beyond the expected superparamagnetic limit ($\sim$100 Gb/in^2) [7] and data rates comparable to those of today's magnetic recording.

The "millipede" concept presented here is a new approach for storing data at high speed and with an ultrahigh density. It is not a modification of an existing storage technology, although the use of magnetic materials as storage medium is not excluded. The ultimate locality is given by a tip, and high data rates are a result of massive parallel operation of such tips. Our current effort is focused on demonstrating the millipede concept with areal densities up to 0.5–1 Tb/in^2 and parallel operation of very large 2-D (32 $\times$ 32) AFM cantilever arrays with integrated tips and write/read storage functionality.

The fabrication and integration of such a large number of mechanical devices (cantilever beams) will lead to what we envision as the VLSI age of micro- and nanomechanics. It is our conviction that VLSI micro/nanomechanics will greatly complement future micro- and nanoelectronics (integrated or hybrid) and may generate applications of VLSI-microelectromechanical systems (MEMS) not conceived of today.

II. Millipede Concept

The 2-D AFM cantilever array storage technique [8] and [9] called "millipede" is illustrated in Fig. 1. It is based on a mechanical parallel x/y scanning of either the entire cantilever array chip or the storage medium. In addition, a feedback-controlled z-approaching and leveling scheme brings the entire cantilever array chip into contact with the storage medium.

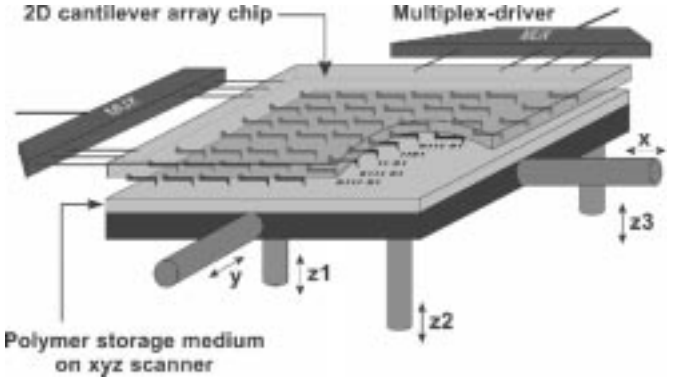

Fig. 1. "Millipede" concept. From [18] and [33].

This tip–medium contact is maintained and controlled while x/y scanning is performed for write/read. It is important to note that the millipede approach is not based on individual z-feedback for each cantilever; rather, it uses a feedback control for the entire chip, which greatly simplifies the system. However, this requires very good control and uniformity of tip height and cantilever bending. Chip approach/leveling makes use of additionally integrated approaching cantilever sensors in the corners of the array chip to control the approach of the chip to the storage medium. Signals from these sensors provide feedback signals to adjust the z-actuators until contact with the medium is established. The system operates similarly to an antivibration table. Feedback loops maintain the chip leveled and in contact with the surface while x/y scanning is performed for write/read operations. This basic concept of the entire chip approach/leveling has been tested and demonstrated for the first time by parallel imaging with a 5 $\times$ 5 array chip [10] and [31]. These parallel imaging results have shown that all 25 cantilever tips have approached the substrate within less than 1 μm of z-activation. This promising result convinced us that chips tip–apex height control of less than 500 nm is feasible. This stringent requirement for tip–apex uniformity over the entire chip is determined by the uniform force required to minimize/eliminate tip and medium wear due to large force variations resulting from large tip-height nonuniformities [4].

During the storage operation, the chip is raster-scanned over an area called the storage field by a magnetic x/y scanner. The scanning distance is equivalent to the cantilever x/y pitch, which is currently 92 μm. Each cantilever/tip of the array writes and reads data only in its own storage field. This eliminates the need for lateral positioning adjustments of the tip to offset lateral position tolerances in tip fabrication. Consequently, a 32 $\times$ 32 array chip will generate 32 $\times$ 32 (1024) storage fields on an area of less than 3 $\times$ 3 mm^2. Assuming an areal density of 500 Gb/in^2, one storage field of 92 $\times$ 92 μm^2 has a capacity of 0.875 MB and the entire 32$\times$32 array with 1024 storage fields has a capacity of 0.9 Gb on 3 $\times$ 3 mm^2. The storage capacity of the system scales with the areal density, the cantilever pitch (storage-field size), and the number of cantilevers in the array. Although not yet investigated in detail, lateral tracking will also be performed for the entire chip with integrated tracking sensors at the chip periphery. This assumes and requires very good temperature control of the array chip

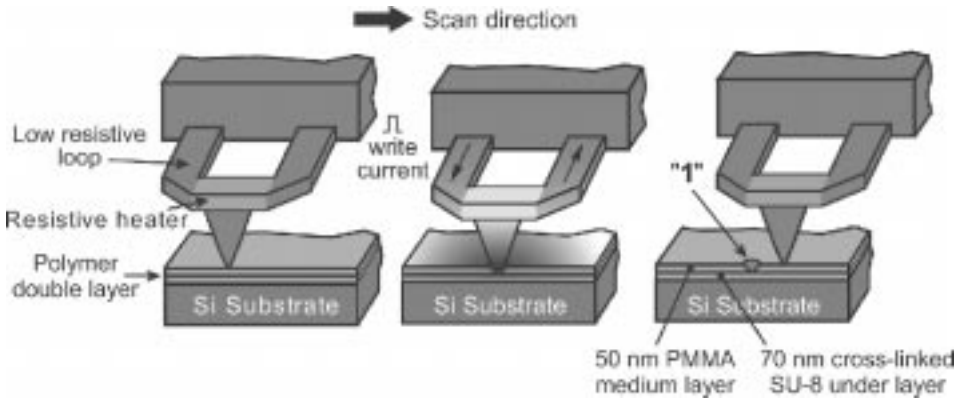

Fig. 2. New storage medium used for writing small bits. A thin writable PMMA layer is deposited on top of a Si substrate separated by a crosslinked film of epoxy photoresist.

and the medium substrate between write and read cycles. For this reason the array chip and medium substrate should be held within about 1 °C operating temperature for bit sizes of 30–40 nm and array chip sizes of a few millimeters. This will be achieved by using the same material (silicon) for both the array chip and the medium substrate in conjunction with four integrated heat sensors that control four heaters on the chip to maintain a constant array-chip temperature during operation. True parallel operation of large 2-D arrays results in very large chip sizes because of the space required for the individual write/read wiring to each cantilever and the many I/O pads. The row/column time-multiplexing addressing scheme implemented successfully in every dynamic random access memory (DRAM) is a very elegant solution to this issue. In the case of millipede, the time-multiplexed addressing scheme is used to address the array row by row with full parallel write/read operation within one row.

The current millipede storage approach is based on a new thermomechanical write/read process in nanometer-thick polymer films, but thermomechanical writing in polycarbonate films and optical readback was first investigated and demonstrated by Mamin and Rugar [2]. Although the storage density of 30 Gb/in^2 obtained originally was not overwhelming, the results encouraged us to use polymer films as well to achieve density improvements.

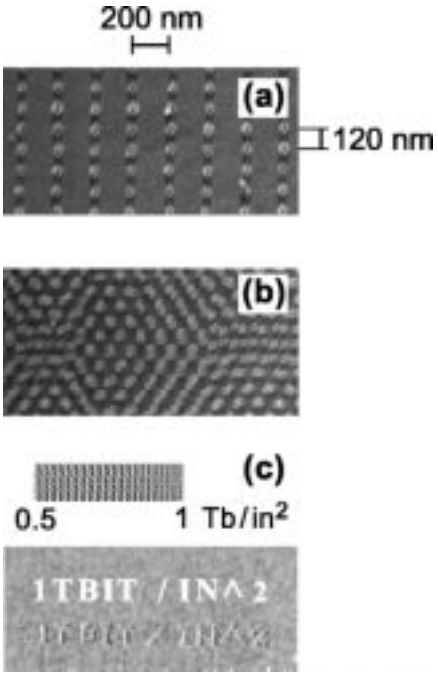

Fig. 3. Series of 40-nm data bits formed in a uniform array with (a) 120-nm pitch and (b) variable pitch ($\geq$40 nm), resulting in bit areal densities of up to 400 Gb/in^2. Images obtained with a thermal read-back technique. (c) Ultrahigh-density bit writing with areal densities approaching 1 Tb/in^2. The scale is the same for all three images.

III. Thermomechanical AFM Data Storage

In recent years, AFM thermomechanical recording in polymer storage media has undergone extensive modifications mainly with respect to the integration of sensors and heaters designed to enhance simplicity and to increase data rate and storage density. Using these heater cantilevers, thermomechanical recording at 30 Gb/in^2 storage density and data rates of a few Mb/s for reading and 100 kb/s for writing have been demonstrated [2], [3], [11]. Thermomechanical writing is a combination of applying a local force by the cantilever/tip to the polymer layer and softening it by local heating. Initially, the heat transfer from the tip to the polymer through the small contact area is very poor and improves as the contact area increases. This means the tip must be heated to a relatively high temperature (about 400 °C) to initiate the softening. Once softening has commenced, the tip is pressed into the polymer, which increases the heat transfer to the polymer, increases the volume of softened polymer, and hence increases the bit size. Our rough estimates [12] and [32] indicate that at the beginning of the writing process only about 0.2% of the heating power is used in the very small contact zone (10–40 nm^2) to soften the polymer locally, whereas about 80% is lost through the cantilever legs to the chip body and about 20% is radiated from the heater platform through the air gap to the medium/substrate. After softening has started and the contact area has increased, the heating power available for generating the indentations increases by at least ten times to become 2% or more of the total heating power.

With this highly nonlinear heat-transfer mechanism it is very difficult to achieve small tip penetration and hence small bit

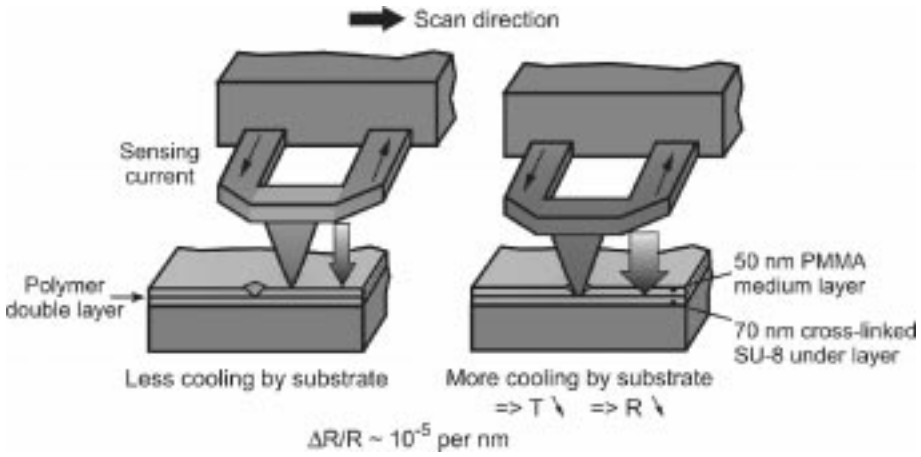

Fig. 4. Principle of AFM thermal sensing. The tip of the heater cantilever is continuously heated by a dc power supply while the cantilever is being scanned and the heater resistivity measured.

sizes as well as to control and reproduce the thermomechanical writing process. This situation can be improved if the thermal conductivity of the substrate is increased, and if the depth of tip penetration is limited. We have explored the use of very thin polymer layers deposited on Si substrates to improve these characteristics [13] and [14], as illustrated in Fig. 2. The hard Si substrate prevents the tip from penetrating farther than the film thickness, and it enables more rapid transport of heat away from the heated region, as Si is a much better conductor of heat than the polymer. We have coated Si substrates with a 40-nm film of polymethylmethacrylate (PMMA) and achieved bit sizes ranging between 10 and 50 nm. However, we noticed increased tip wear, probably caused by the contact between Si tip and Si substrate during writing. We, therefore, introduced a 70-nm layer of crosslinked photoresist (SU-8) between the Si substrate and the PMMA film to act as a softer penetration stop that avoids tip wear, but remains thermally stable.

Using this layered storage medium, data bits 40 nm in diameter have been written as shown in Fig. 3. These results were performed using a 1-μm-thick, 70-μm-long, two-legged Si cantilever [11]. The cantilever legs are made highly conducting by high-dose ion implantation, whereas the heater region remains low doped. Electrical pulses 2 μs in duration were applied to the cantilever with a period of 50 μs. Fig. 3(a) demonstrates that 40-nm bits can be written with 120-nm pitch or very close to each other without merging [Fig. 3(b)], implying a potential bit areal density of 400 Gb/in^2. More recently we have demonstrated single-cantilever areal densities up to 1 Tb/in^2, although currently at a somewhat degraded write/read quality [Fig. 3(c)].

Imaging and reading are done using a new thermomechanical sensing concept [15]. The heater cantilever originally used only for writing was given the additional function of a thermal readback sensor by exploiting its temperature-dependent resistance. The resistance (R) increases nonlinearly with heating power/temperature from room temperature to a peak value of 500 °C–700 °C. The peak temperature is determined by the doping concentration of the heater platform, which ranges from 1×10^{17} to 2×10^{18}. Above the peak temperature, the resistance drops as the number of intrinsic carriers increases because of thermal excitation [16]. For sensing, the resistor is operated

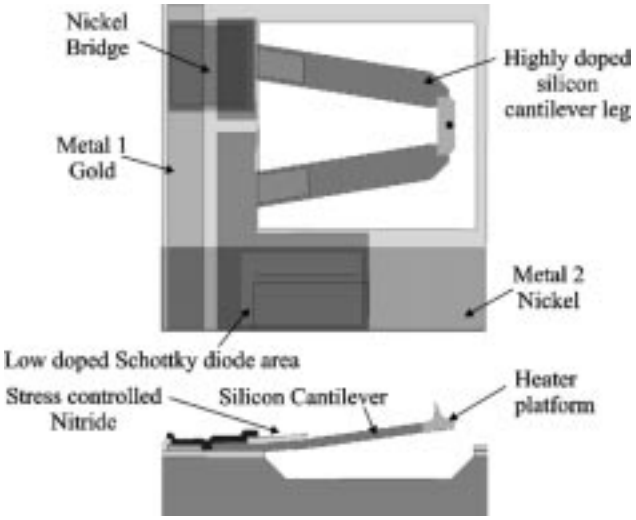

Fig. 5. Layout and cross section of one cantilever cell. From [18] and [33].

at about 350 °C, a temperature that is not high enough to soften the polymer as is the case for writing. The principle of thermal sensing is based on the fact that the thermal conductance between the heater platform and the storage substrate changes according to the distance between them. The medium between a cantilever and the storage substrate—in our case air—transports heat from one side to the other. When the distance between heater and sample is reduced as the tip moves into a bit indentation, the heat transport through air will be more efficient, and the heater's temperature and hence its resistance will decrease. Thus, changes in temperature of the continuously heated resistor are monitored while the cantilever is scanned over data bits, providing a means of detecting the bits. Fig. 4 illustrates this concept.

Under typical operating conditions, the sensitivity of thermomechanical sensing is even better than that of piezoresistive-strain sensing, which is not surprising because thermal effects in semiconductors are stronger than strain effects. The good $\Delta R/R$ sensitivity of about 10^{-5}/nm is demonstrated by the images of the 40-nm-size bit indentations in Fig. 3, which have been obtained using the described thermal-sensing technique.

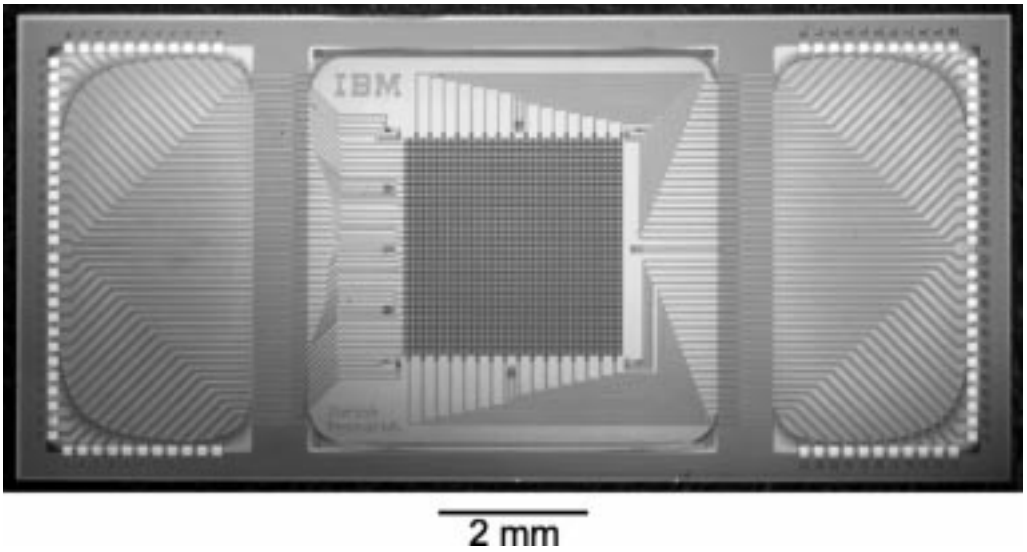

Fig. 6. Photograph of fabricated chip (14 × 7 mm^2). The 32 × 32 cantilever array is located at the center, with bond pads distributed on either side. From [18] and [33].

IV. Array Design, Technology, Fabrication

Encouraged by the results of the 5 × 5 cantilever array [10] and [31], we designed and fabricated a 32 × 32 array chip. With the findings from the fabrication and operation of the 5 × 5 array and the very dense thermomechanical writing/reading in thin polymers with single cantilevers, we made some important changes in the chip functionality and fabrication processes. The major differences are: 1) surface micromachining to form cantilevers at the wafer surface; 2) all-silicon cantilevers; 3) thermal instead of piezoresistive sensing; and 4) first- and second-level wiring with an insulating layer for a multiplexed row/column-addressing scheme.

As the heater platform functions as a read/write element and no individual cantilever actuation is required, the basic array cantilever cell becomes a simple two-terminal device addressed by a multiplexed x/y wiring as shown in Fig. 5. The cell area and x/y cantilever pitch are 92 × 92 μm^2, which results in a total array size of less than 3 × 3 mm^2 for the 1024 cantilevers. The cantilevers are fabricated entirely of silicon for good thermal and mechanical stability. They consist of a heater platform with the tip on top, legs acting as a soft mechanical springs, and electrical connections to the heater. They are highly doped to minimize interconnect resistance and to replace the metal wiring on the cantilever in order to eliminate electromigration and parasitic z-actuation of the cantilever due to a bimorph effect. The resistive ratio between the heater and the silicon interconnect sections should be as high as possible; currently the resistance of the highly doped interconnections is ∼400 Ω and that of the heater platform is 5-kΩ (at 3 V reading bias).

The cantilever mass has to be minimized to obtain soft, high-resonant-frequency cantilevers. Soft cantilevers are required for a low loading force in order to eliminate or reduce tip and medium wear, whereas a high resonant frequency allows high-speed scanning. In addition, sufficiently wide cantilever legs are required for a small thermal time constant, which is partly determined by cooling via the cantilever legs [11]. These design considerations led to an array cantilever with 50-μm-long, 10-μm-wide, and 0.5-μm-thick legs, and a 5-μm-wide, 10-μm-long, and 0.5-μm-thick platform. Such a cantilever has a stiffness of ∼1 N/m and a resonant frequency of ∼200 kHz. The heater time constant is a few microseconds, which should allow a multiplexing rate of up to 100 kHz.

The tip height should be as small as possible because the heater platform sensitivity strongly depends on the platform-to-medium distance. This contradicts the requirement of a large gap between the chip surface and the storage medium to ensure that only the tips, and not the chip surface, are making contact with the medium. Instead of making the tips longer, we purposely bent the cantilevers a few micrometers out of the chip plane by depositing a stress-controlled plasma-enhanced chemical vapor deposition (PECVD) silicon-nitride layer at the base of the cantilever (see Fig. 5). This bending as well as the tip height must be well controlled in order to maintain an equal loading force for all cantilevers of an array.

Cantilevers are released from the crystalline Si substrate by surface micromachining using either plasma or wet chemical etching to form a cavity underneath the cantilever. Compared to a bulk-micromachined through-wafer cantilever-release process as done for our 5 × 5 array [10] and [31], the surface-micromachining technique allows an even higher array density and yields better mechanical chip stability and heat sinking. As the millipede tracks the entire array without individual lateral cantilever positioning, thermal expansion of the array chip has to be small or well controlled. Because of thermal chip expansion, the lateral tip position must be controlled with better precision than the bit size, which requires array dimensions as small as possible and a well-controlled chip temperature. For a 3 × 3 mm^2 silicon array area and 10-nm tip-position accuracy, the chip temperature has to be controlled to about 1 °C. This is ensured by four temperature sensors in the corners of the array and heater elements on each side of the array. Thermal expansion considerations were a strong argument for the 2-D array arrangement instead of 1-D, which would have made the chip 32 times longer for the same number of cantilevers.

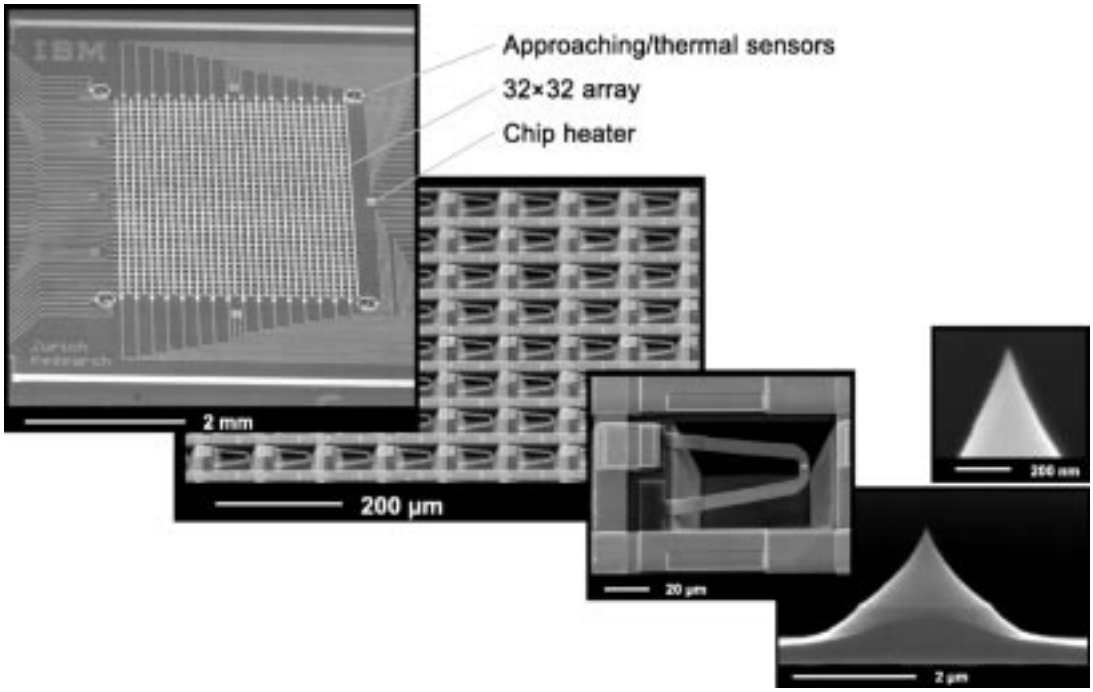

Fig. 7. SEM images of the cantilever array section with approaching and thermal sensors in the corners, array and single cantilever details, and tip apex. Copyright 2000 by International Business Machines Corporation; reprinted with permission from the IBM Journal of Research and Development [19].

The photograph in Fig. 6 shows a fabricated chip with the 32×32 array located in the center (3×3 mm^2) and the electrical wiring interconnecting the array with the bonding pads at the chip periphery.

Fig. 7 shows the 32×32 array section of the chip with the independent approach/heat sensors in the four corners and the heaters on each side of the array as well as zoomed scanning electron micrographs (SEMs) of an array section, a single cantilever, and a tip apex. The tip height is 1.7 μm and the apex radius is smaller than 20 nm, which is achieved by oxidation sharpening [17].

The cantilevers are connected to the column and row address lines using integrated Schottky diodes in series with the cantilevers. The diode is operated in reverse bias (high resistance) if the cantilever is not addressed, thereby greatly reducing crosstalk between cantilevers. More details about the array fabrication are given in [18] and [33].

V. Array Characterization

The array's independent cantilevers, which are located in the four corners of the array and used for approaching and leveling of chip and storage medium, are used to initially characterize the interconnected array cantilevers. Additional cantilever test structures are distributed over the wafer; they are equivalent to but independent of the array cantilevers. Fig. 8 shows an I–V curve of such a cantilever; note the nonlinearity of the resistance. In the low-power part of the curve, the resistance increases as a function of heating power, whereas in the high-power regime, it decreases.

In the low-power, low-temperature regime, silicon mobility is affected by phonon scattering, which depends on temperature, whereas at higher power the intrinsic temperature of the semiconductor is reached, which results in a resistivity drop owing to the increasing number of carriers [16]. Depending on the heater-platform doping concentration of 1×10^{17} to 2×10^{18} at/cm^3, our calculations estimate a resistance maximum at a temperature of 500 °C–700 °C, respectively.

The cantilevers within the array are electrically isolated from one another by integrated Schottky diodes. As every parasitic path in the array to the cantilever addressed contains a reverse-biased diode, the crosstalk current is drastically reduced as shown in Fig. 9. Thus, the current response to an addressed cantilever in an array is nearly independent of the size of the array, as demonstrated by the I/V curves in Fig. 9. Hence, the power applied to address a cantilever is not shunted by other cantilevers, and the reading sensitivity is not degraded—not even for very large arrays (32×32). The introduction of the electrical isolation using integrated Schottky diodes turned out to be crucial for the successful operation of interconnected cantilever arrays with a simple time-multiplexed addressing scheme.

The tip–apex height uniformity within an array is very important, because it determines the force of each cantilever while in contact with the medium and hence influences write/read performance as well as medium and tip wear. Wear investigations suggest that a tip–apex height uniformity across the chip of less than 500 nm is required [4], with the exact number depending on the spring constant of the cantilever. In the case of the millipede, the tip–apex height is determined by the tip height and the cantilever bending. Fig. 10 shows the tip–apex height uniformity of one row of the array (32 tips) due to tip height and cantilever bending. It demonstrates that our uniformity is on the order of 100 nm, thus, meeting the requirements.

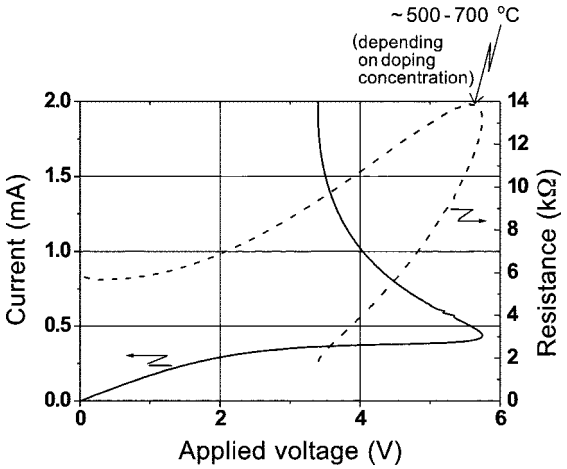

Fig. 8. I/V curve of one cantilever. The curve is nonlinear owing to the heating of the platform as the power and temperature are increased. For doping concentrations between 1×10^{17} and 2×10^{18} at/cm^3, the maximum temperature varies between 500 and 700 °C. Reprinted [33], by permission of Elsevier Science.

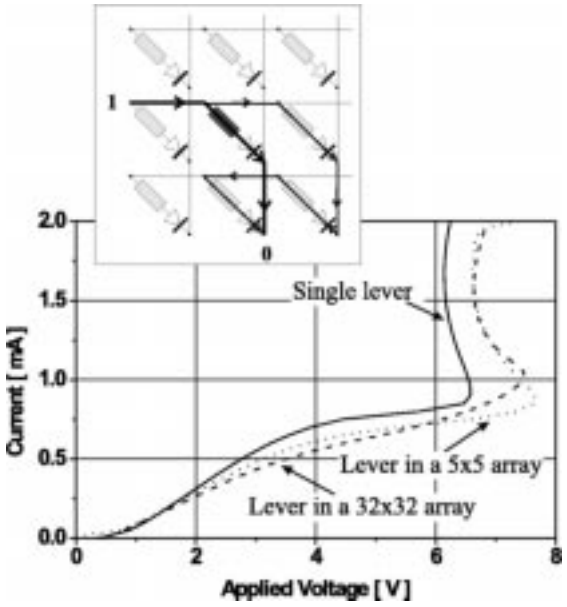

Fig. 9. Comparison of the I/V curve of an independent cantilever (solid line) with the current response when addressing a cantilever in a 5×5 (dotted line) or a 32×32 (dashed line) array with a Schottky diode serially to the cantilever. Little change is observed in the I/V curve between the different cases. Also shown in the inset is a sketch representing the direct path (thick line) and a parasitical path (thin line) in a cantilever–diode array. In the parasitical path there is always one diode in reverse bias that reduces the parasitical current. Reprinted from [33], by permission of Elsevier Science.

VI. $x/y/z$ Media Microscanner

A key issue for the millipede concept is the need for a low-cost, miniaturized scanner with $x/y/z$ motion capabilities and a lateral scanning range on the order of 100 μm. Multiple-probe systems arranged as 1-D or 2-D arrays [19] must also be able to control, by tilt capabilities, the parallelism between the probe array and the sample [19] and [20].

We have developed a microscanner with these properties based on electromagnetic actuation. It consists of a mobile platform, supported by springs and containing integrated planar coils, which are positioned over a set of miniature permanent magnets [21]. A suitable arrangement of the coils and magnets allows us, by electrically addressing the different coils, to apply magnetically induced forces to the platform and drive it in the x, y, z, and tilt directions. Our first silicon/copper-based version of this device has proved the validity of the concept [22], and variations of it have since been used elsewhere [23]. However, the undamped copper spring system gave rise to excessive cross talk and ringing when driven in an open loop, and its layout limited the compactness of the overall device.

We investigate a modified microscanner that uses flexible rubber posts as a spring system and a copper–epoxy-based mobile platform, Fig. 11. The platform is made of a thick, epoxy-based SU-8 resist [24], in which the copper coils are embedded. The posts are made of polydimethylsiloxane (PDMS) [25] and are fastened at the corners of the platform and at the ground plate, providing an optimally compact device by sharing the space below the platform with the magnets. The shape of the posts allows their lateral and longitudinal stiffness to be adjusted, and the dissipative rubber-like properties of PDMS provide damping to avoid platform ringing and to suppress nonlinearities.

Fig. 12 shows the layout of the platform, which is scaled laterally so that the long segments of the "racetrack" coils used for in-plane actuation coincide with commercially available 24 mm^2 SmCo magnets. The thickness of the device is determined by that of the magnets (1 mm), the clearance between magnet and platform (500 μm), and the thickness of the platform itself, which is 250 μm and determined mainly by the aspect ratio achievable in SU-8 resist during the exposure of the coil plating mold. The resulting device volume is approximately $15 \times 15 \times 1.6$ mm^3.

The SmCo magnets produce a measured magnetic field intensity of $\simeq$0.14 T at the mid-thickness of the coils. The effective coil length is 320 mm, yielding an expected force $F_{x,y}$ of 45 μN per milliamp of drive current.

The principal design issue of the spring system is the ratio of its stiffnesses for in-plane and out-of-plane motion. Whereas for many scanning probe applications the required z axis range need not be much larger than a few microns, it is necessary to ensure that the z axis retraction of the platform due to the shortening of the posts as they take on an "S"-shape at large in-plane deflections can be compensated for at acceptable z-coil current levels. Various PDMS post shapes have been investigated to optimize and trade off the different requirements. Satisfactory performance was found for simple O-shapes [26].

The fabrication of the scanner, Fig. 13, starts on a silicon wafer with a seed layer and a lithographically patterned 200-μm-thick SU-8 layer, in which copper is electroplated to form the coils [Fig. 13(a)]. The coils typically have 20 turns, with a pitch of 100 μm and a spacing of 20 μm. Special care was taken in the resist processing and platform design to achieve the necessary aspect ratio and to overcome adhesion and stress problems of SU-8. A second SU-8 layer, which serves as an insulator, is patterned with via holes, and another seed layer is then deposited [Fig. 13(b)]. Next, an interconnect level is formed using a Novolac-type resist mask and a second copper-electroplating step [Fig. 13(c)]. After stripping the resist, the silicon wafer is dissolved by a sequence of wet and

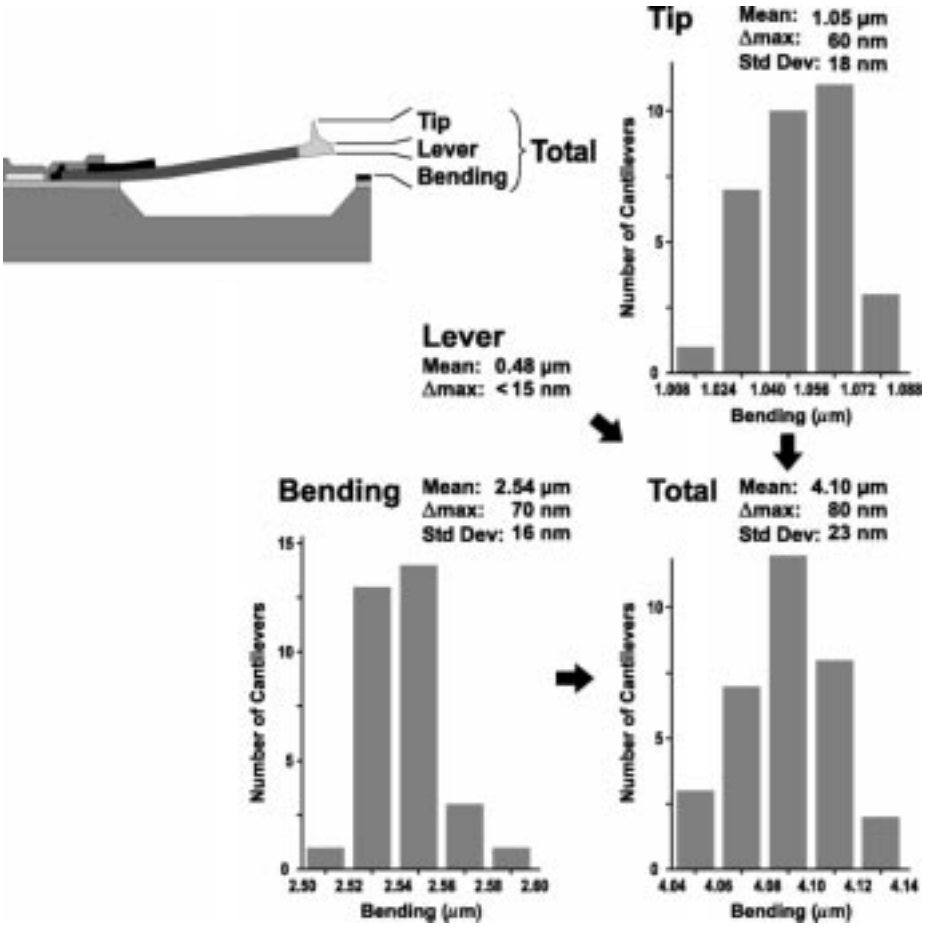

Fig. 10. Tip–apex height uniformity across one cantilever row of the array with individual contributions from the tip height and cantilever bending. Copyright 2000 by International Business Machines Corporation; reprinted with permission from the IBM Journal of Research and Development [19].

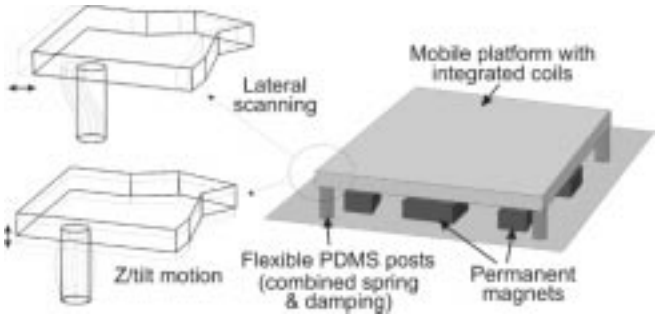

Fig. 11. Microscanner concept, using a mobile platform and flexible posts. From [26].

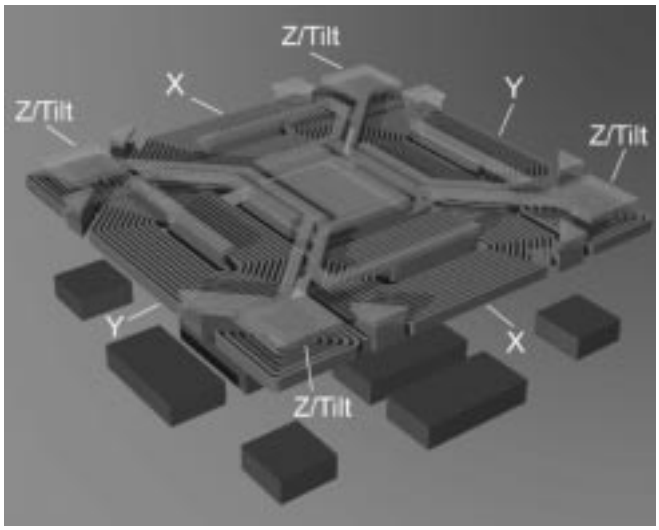

Fig. 12. Arrangement of the coils, the interconnects and the permanent magnets, as well as the various motions addressed by the corresponding coils.

dry etching, and the exposed seed layers are sputtered away to prevent shorts [Fig. 13(d)].

The motion of the scanner was characterized using a microvision strobe technique[1] [27]. The results presented below are based on O-type PDMS posts. Frequency response curves for in-plane motion (Fig. 14) show broad peaks (characteristic of a large degree of damping) at frequency values that are consistent with expectations based on the measured mass of the platform (0.253 mg). The amplitude response (Fig. 15) displays the excellent linearity of the spring system for displacement amplitudes up to 80 μm (160-μm displacement range). Based on these near-dc (10 Hz) responses ($\sim$1.4-μm/mA), and a measured circuit resistance of 1.9 Ω, the power necessary for a 50-μm displacement amplitude is $\sim$2.5 mW.

[1]The equipment used is a Networked Probe Station from Umech Technologies, Cambridge, MA.

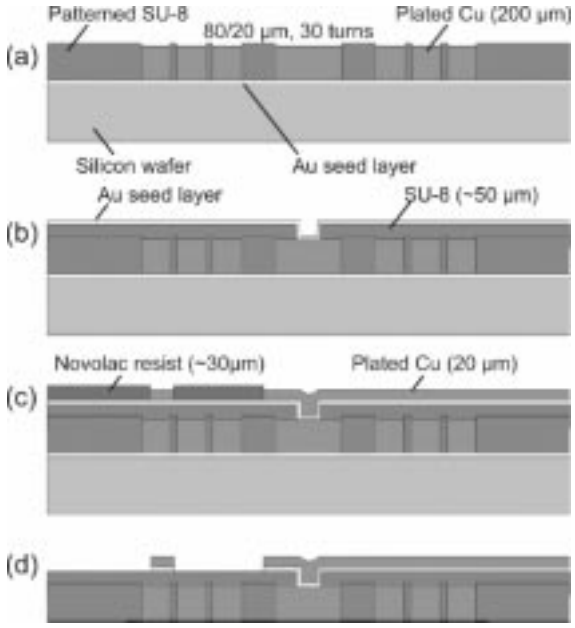

Fig. 13. Cross section of the platform-fabrication process. (a) Coils are electroplated through an SU-8 resist mask, which is retained as the body of the platform. (b) Insulator layer is deposited. (c) Interconnects are electroplated. (d) Platform is released from the silicon substrate. From [26].

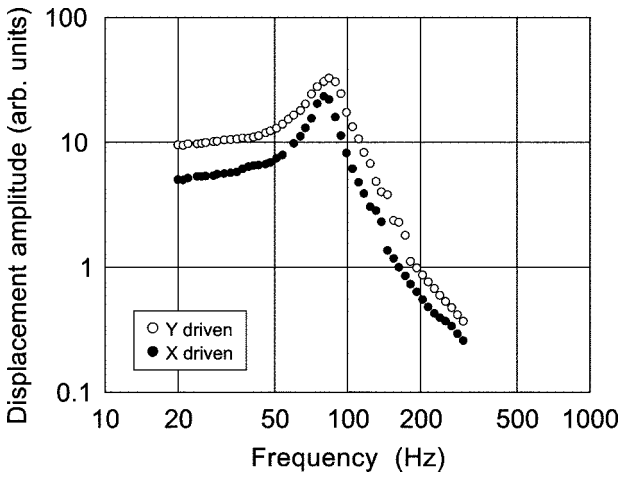

Fig. 14. Frequency response for in-plane x and y axis. The mechanical quality factors measured are between 3.3 and 4.6.

Owing to limitations of the measurement technique, it was not possible to measure out-of-plane displacements greater than 0.5 μm. However, the small-amplitude response for z-motion when all four corner coils are driven in-phase also displays good linearity over the range that can be measured (Fig. 16).

The electromagnetic scanner performs as predicted and reliably in terms of the scan range, device volume, and power requirements, achieving overall displacement ranges of 100 μm with approximately 3 mW of power. The potential access time in the 100-μm storage field is on the order of a few milliseconds. By being potentially cheap to manufacture, the integrated scanner presents a good alternative actuation system for many scanning probe applications.

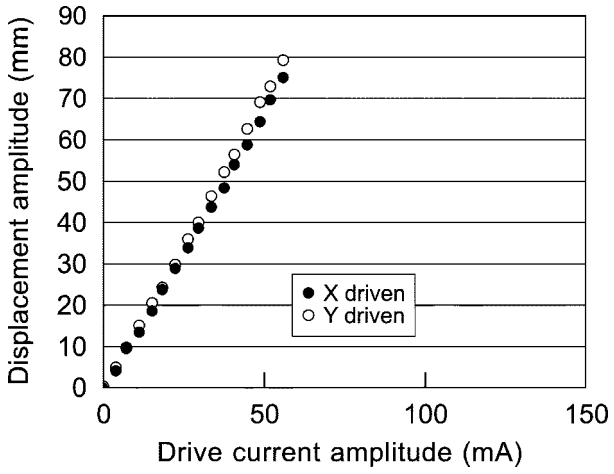

Fig. 15. In-plane displacement amplitude response for an ac drive current at 10 Hz (off resonance).

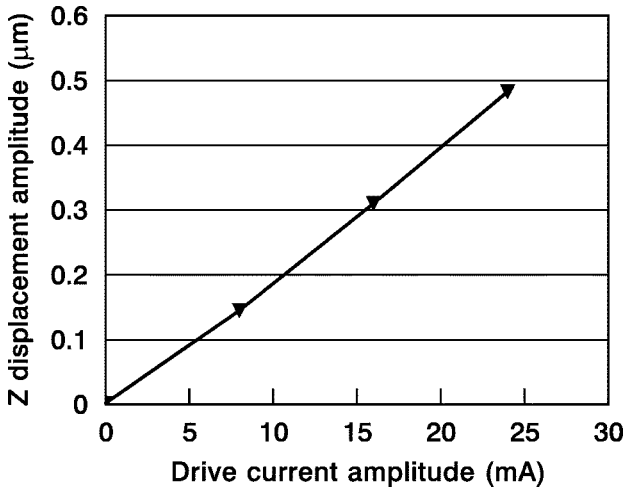

Fig. 16. Out-of-plane amplitude response for an ac drive current at 3 Hz. The drive current is the total for all four corner coils, which are driven in phase. From [26].

VII. First Write/Read Results With the 32 × 32 Array Chip

We have built a research demonstration that includes all basic building blocks of the millipede concept (see Fig. 1) [28]. A 3 × 3 mm^2 silicon substrate is spin-coated with the SU-8/PMMA polymer medium as described in Section III. This storage medium is attached to the $x/y/z$ micro-scanner and approaching device. The magnetic z-approaching actuators bring the medium into contact with the tips of the array chip. The z-distance between medium and the millipede chip is controlled by the approaching sensors in the corners of the array. The signals from these cantilevers are used to determine the forces on the z-actuators and, hence, also the forces of the cantilever while it is in contact with the medium. This sensing/actuation feedback loop continues to operate during x/y scanning of the medium. The PC-controlled write/read scheme addresses the 32 cantilevers of one row in parallel. Writing is performed by connecting the addressed row for 20 μs to a high, negative voltage and simultaneously applying data inputs ("0" or "1") to the 32 column lines. The data input

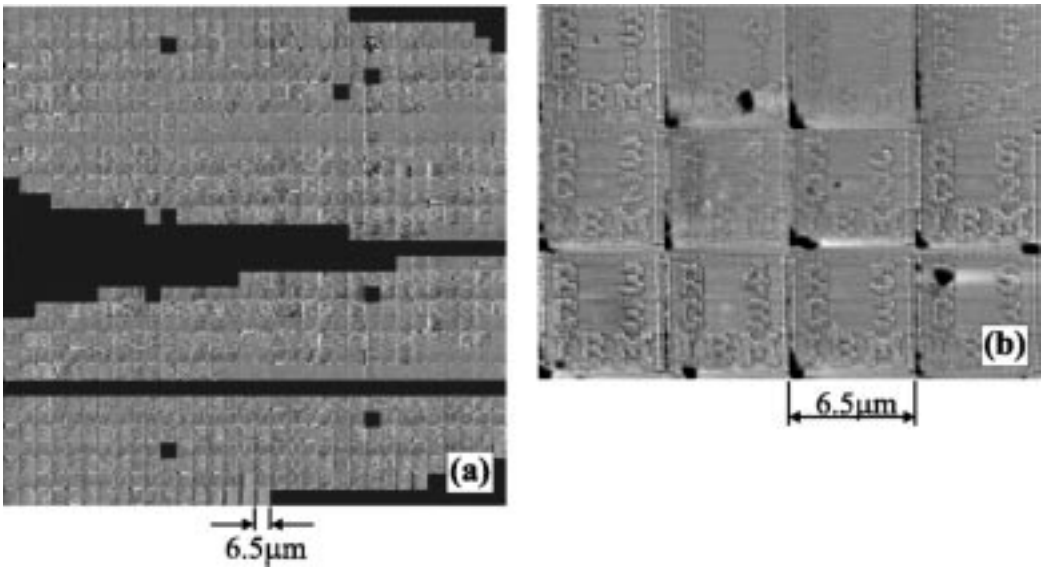

Fig. 17. (a) 1024 images, one from each lever at 15–30 Gb/in^2. (b) Enlarged view of typical images from (a). Numbers in the images indicate the row and column of each lever. From [28].

is a high, positive voltage for a "1" and ground for a "0." This row-enabling and column-addressing scheme supplies a heater current to all cantilevers, but only those cantilevers with high, positive voltage generate an indentation ("1"). Those with ground are not hot enough to make an indentation, and, thus, write a "0." When the scan stage has moved to the next bit position, the process is repeated, and this is continued until the line scan is finished. In the read process, the selected row line is connected to a moderate negative voltage, and the column lines are grounded via a protection resistor of about 10 kΩ, which keeps the cantilevers warm. During scanning, the voltages across the resistors are measured. If one of the cantilevers falls into a "1" indentation, it cools, thus, changing the resistance and voltage across the series resistor and allowing written data bits to be read back.

The results of writing and reading in this fashion can be seen in Fig. 17, which shows 1024 images written by the levers then read back. Of the 1024 levers, 834 were able to write and read back data, which is more than 80%. The sequence is as follows. First a bit pattern is written to each of the levers in row 1 simultaneously then read back simultaneously, followed by row 2, etc., until row 32. The images sent to the levers are different, each lever writing its own row and column number in the array. The bit pattern is 64 $\times$ 64 bits, but odd bits are always 0. In this case the area used is 6.5 $\times$ 6.5 μm^2. The image read back is a gray-scale bit map of 128 $\times$ 128 pixels. The interlever distance is 92 μm, so the images in Fig. 17 are also 92 μm apart. A working storage system would fill the entire space between levers with data. The data in Fig. 17 correspond to 15–30 Gb/in^2, depending on whether the coding system allows adjacent bits to run together. More recently, we have demonstrated 150–200 Gb/in^2 at an array yield of about 60%.

Those levers that did not read back failed for one of four reasons: 1) a defective chip connector like that in column 25 made that column unusable; 2) a point defect occurred, meaning that a single lever or tip is broken; 3) nonuniformity of the tip contact due to tip/lever variability or storage substrate bowing due to mounting; and 4) thermal drifts, with the latter two being the most likely and major failure sources.

At present, there is clearly a tradeoff between the number of working levers and the density, which will most likely be resolved by a better substrate/chip mounting technique and lower thermal drifts.

The writing and readback rates achieved with this system are 1 kb/s/lever, thus, the total data rate is about 32 kb/s. This rate is limited by the rate at which data can be transferred over the PC ISA bus, not by a fundamental time limitation of the read/write process.

VIII. Polymer Medium

The polymer storage medium plays a crucial role in millipede-like thermomechanical storage systems. The thin-film-sandwich structure with PMMA as active layer (see Fig. 2) is not the only choice possible, considering the almost unlimited range of polymer materials available. The ideal medium should be easily deformable for bit writing, yet written bits should be stable against tip wear and thermal degradation. Finally, one would also like to be able to repeatedly erase and rewrite bits. In order to be able to scientifically address all important aspects, some understanding of the basic physical mechanism of thermo-mechanical bit writing and erasing is required.

In a gedanken experiment we visualize bit writing as the motion of a rigid body, the tip, in a viscous medium, the polymer melt. For the time being, the polymer, i.e., PMMA, is assumed to behave like a simple liquid after it has been heated above the glass-transition temperature in a small volume around the tip. As viscous drag forces must not exceed the loading force applied to the tip during indentation, we can estimate an upper bound for the viscosity η of the polymer melt using Stokes' equation

$$F = 6\pi\eta R v. \tag{1}$$

In actual millipede bit writing, the tip loading force is on the order $F = 50$ nN, and the radius of curvature at the apex of the

tip is typically $R = 20$ nm. Assuming a depth of the indentation of, say, $h = 50$ nm and a heat pulse of $\tau_h = 10$ μs duration, the mean velocity during indentation is on the order of $v = h/\tau_h = 5$ mm s^{-1} (note that thermal relaxation times are of the order of microseconds [12] and [32], and hence the heating time can be equated to the time it takes to form an indentation). With these parameters we obtain $\eta < 25$ Pa s, whereas typical values for the shear viscosity of PMMA are at least seven orders of magnitude larger even at temperatures well above the glass-transition point [29].

This apparent contradiction can be resolved by considering that polymer properties are strongly dependent on the time scale of observation. At time scales of the order of 1 ms and below, entanglement motion is in effect frozen in and the PMMA molecules form a relatively static network. Deformation of the PMMA now proceeds by means of uncorrelated deformations of short molecular segments rather than by a flow mechanism involving the coordinated motion of entire molecular chains. The price one has to pay is that elastic stress builds up in the molecular network as a result of the deformation (the polymer is in a so-called rubbery state). On the other hand, corresponding relaxation times are orders of magnitude smaller, giving rise to an effective viscosity at millipede time scales of the order of 10 Pa s [29] as required by our simple argument [see (1)]. Note that, unlike the normal viscosity, this high-frequency viscosity is basically independent of the detailed molecular structure of the PMMA, i.e., chain length, tacticity, poly-dispersity, etc. In fact, we can even expect that similar high-frequency viscous properties are found in a large class of other polymer materials, which makes thermomechanical writing a rather robust process in terms of material selection.

We have argued above that elastic stress builds up in the polymer film during indentation, creating a corresponding reaction force on the tip of the order of $F_r \sim 2\pi GR^2$, where G denotes the elastic shear modulus of the polymer.[2] An important property for millipede operation is that the shear modulus drops by orders of magnitude in the glass-transition regime, i.e., for PMMA from $\sim$1 GPa below T_g to $\sim 0.5 \cdots 1$ MPa above T_g [29]. (The bulk modulus, on the other hand, retains its low-temperature value of several GPa. Hence, in this elastic regime, formation of an indentation above T_g constitutes a volume-preserving deformation.) For proper bit writing, the tip load must be balanced between the extremes of the elastic reaction force F_r for temperatures below and above T_g, i.e., for PMMA $F \ll 2.5$ μN to prevent indentation of the polymer in the cold state and $F \gg 2.5$ nN to overcome the elastic reaction force in the hot state. Unlike the deformation of a simple liquid, the indentation represents a metastable state of the entire deformed volume, which is under elastic tension. Recovery of the unstressed initial state is prevented by rapid quenching of the indentation below the glass temperature with the tip in place. As a result, the deformation is frozen in because below T_g motion of molecular-chain segments is effectively inhibited (see Fig. 18).

This mechanism also allows local erasing of bits—it suffices to locally heat the deformed volume above T_g whereupon the indented volume reverts to its unstressed flat state driven by internal elastic stress. In addition, erasing is promoted by surface

[2]The estimate is based on a fluid dynamic deformation model of a thin film.

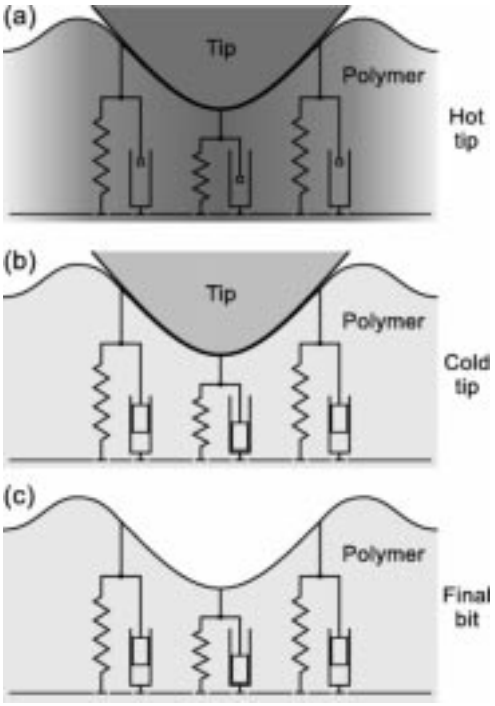

Fig. 18. Visco-elastic model of bit writing. (a) The hot tip heats a small volume of polymer material to more than T_g: the shear modulus of the polymer drops drastically from GPa to MPa, which in turn allows the tip to indent the polymer. In response, elastic stress (represented as compression springs) builds up in the polymer. In addition, viscous forces (represented as pistons) associated with the relaxation time for the local deformation of molecular segments limit the indentation speed. (b) At the end of the writing process, the temperature is quenched on a microsecond time scale to room temperature: the stressed configuration of the polymer is frozen-in (represented by the locked pistons). (c) The final bit corresponds to a metastable configuration. The original unstressed flat state of the polymer can be recovered by heating the bit volume to more than T_g, which unlocks the compressed springs.

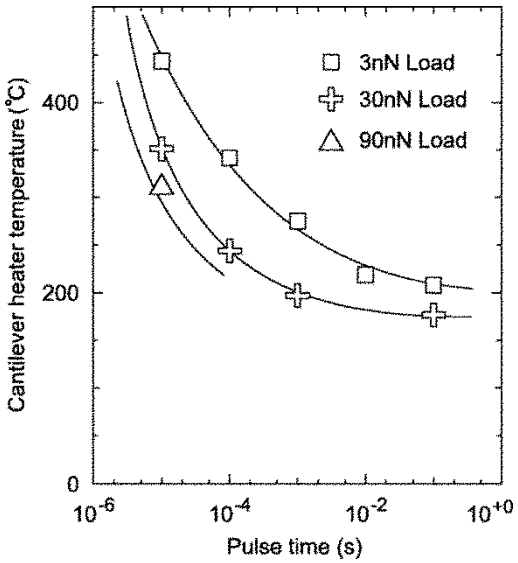

Fig. 19. Bit-writing threshold measurements. The load was controlled by pushing the cantilever/tip into the sample with a controlled displacement and a known spring constant of the cantilever. When a certain threshold is reached, the indentations become visible in subsequent imaging scans (see also Fig. 21). The solid lines are guides to the eye. Curves of similar shape would be expected from the time–temperature superposition principle.

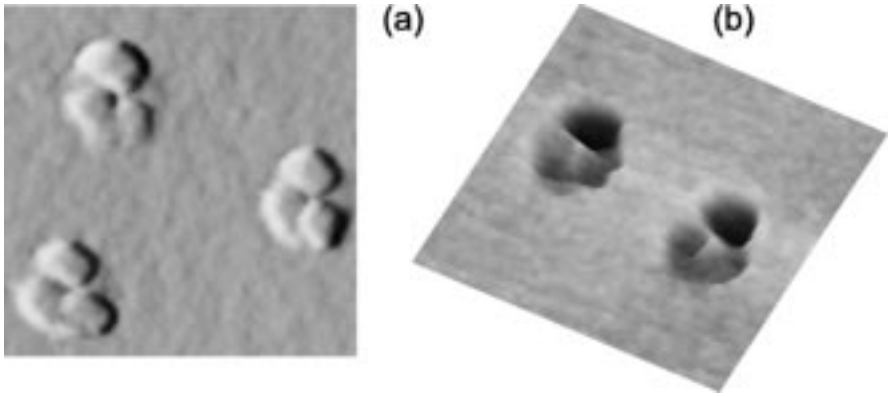

Fig. 20. Topographic image of individual bits. (a) Region around the actual indentations clearly shows the three-fold symmetry of the tip, here a three-sided pyramid. (b) Indentations themselves exhibit sharp edges, as can be seen from the inverted 3-D image. Image size is 2 μm.

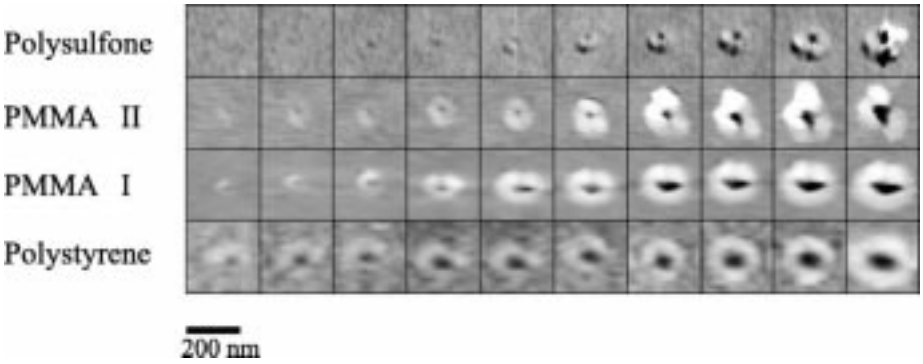

Fig. 21. Written bits for different polymer materials. The heating pulse length was 10 μs, the load about 10 nN. The gray scale is the same for all images. The heater temperatures for the bit on the left-hand side are 445, 400, 365, and 275 °C for the polymers Polysulfone, PMMA II (anionically polymerized PMMA, $M \simeq 26$ k), PMMA I (Polymer Standard Service (Germany) $M \simeq 500$ k), and Polystyrene, respectively. The temperature increase between events on the horizontal axis was 14, 22, 20, and 9 °C, respectively.

tension forces, which give rise to a restoring surface pressure on the order of $\gamma(\pi/R)^2 h \sim 25$ MPa, where $\gamma \sim 0.02$ Nm^{-1} denotes the polymer–air surface tension.

One question immediately arises from these speculations: If the polymer behavior can be determined from the macroscopic characteristics of the shear modulus as a function of time, temperature, and pressure, can then the time–temperature superposition principle also be applied in our case? The time–temperature superposition principle is a very successful concept of polymer physics [30]. It basically says that the time scale and the temperature are interdependent variables that determine the polymer behavior such as the shear modulus. A simple transformation can be used to translate time-dependent into temperature-dependent data and vice versa. It is not clear, however, whether this principle can be applied in our case, i.e., under such extreme conditions (high pressures, short time scales and nanometer-sized volumes, which are clearly below the radius of gyration of individual polymer molecules).

To test this, we varied the heating time, the heating temperature, and the loading force in bit-writing experiments on a standard PMMA sample. The results are summarized in Fig. 19. The minimum heater temperature at which bit formation starts for a given heating-pulse length and loading force was determined. This so-called threshold temperature is plotted against the heating-pulse length. A careful calibration of the heater temperature has to be done to allow a comparison of

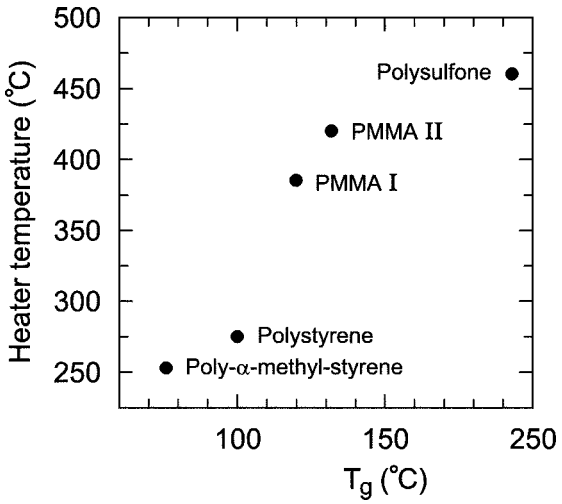

Fig. 22. The heater temperature threshold for writing bits with the same parameters as in Fig. 21 is plotted against the glass-transition temperature for these polymers including poly-α–methyl–styrene.

the data. The heater temperature was determined by assuming proportionality between temperature and electrical power dissipated in the heater resistor at the end of the heating pulse when the tip has reached its maximum temperature. An absolute temperature scale is established using two well-defined reference points. One is room temperature, corresponding to

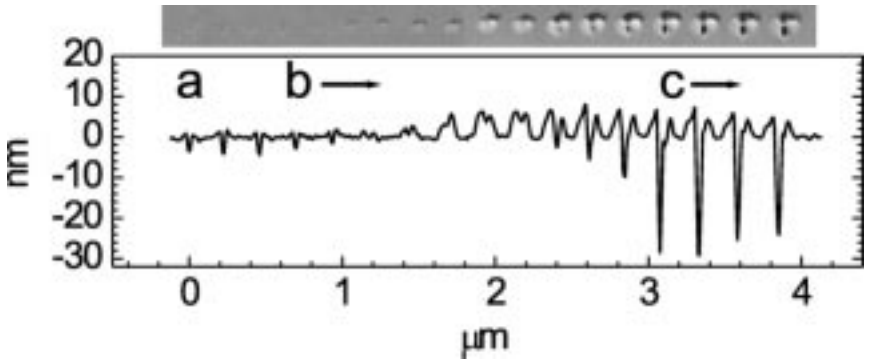

Fig. 23. Section through a series of bits similar to Fig. 21. Here, a load of about 200 nN was applied before a heating pulse of 10-μs length was fired. The temperature of the heater at the end of the pulse has been increased from 430 to 610 °C in steps of about 10.6 °C. (a) Load was sufficient to form a plastic indentation even if the polymer is not heated enough to come near the glass transition. (b) By increasing the heater temperature a swelling of the polymer occurs which works against the indentation and leads to an erasure of previously written "cold" bits. (c) As this process continues, the thermomechanical formation of indentations begins to dominate until, finally, normal thermomechanical bit writing occurs.

zero electrical power. The other is provided by the point of turnover from positive to negative differential resistance (see Fig. 8), which corresponds to a heater temperature of 550 °C. The general shape of the measured threshold-temperature versus heating-time curves indeed shows the characteristics of time-temperature superposition. In particular, the curves are identical up to a load-dependent shift with respect to the time axis. Moreover we observe that at constant heater temperature the time it takes to write a bit is inversely proportional to the tip load. This property is exactly what one would expect if internal friction (owing to the high-frequency viscosity) is the rate-limiting step in bit writing [see (1)].

The time it takes to heat the bit volume of polymer material to more than the glass-transition temperature is another potentially rate-limiting step. Here the spreading resistance of the heat flow in the polymer and the thermal contact resistance are the most critical parameters. Simulations suggest [12] and [32] that equilibration of temperature in the polymer occurs within less than 1 μs. Very little is known, however, on the thermal coupling efficiency across the tip-polymer interface. We have several indications that the heat transfer between tip and sample plays a crucial role, one of them being the asymptotic heater temperature for long writing times, which according to the graph (Fig. 19) is approximately 200 °C. The exact temperature of the polymer is unknown. However, the polymer temperature should approach the glass-transition temperature (around 120 °C for PMMA) asymptotically. Hence, the temperature drop between heater and polymer medium is substantial. Part of the temperature difference is due to a temperature drop along the tip, which according to heat-flow simulations [12] and [32] is expected to be on the order of 30 °C at most. Therefore, a significant temperature gradient must exist in the tip-polymer contact zone. Further experiments on the heat transfer from tip to surface are needed to clarify this point.

We also find that the heat transfer for a nonspherical tip is anisotropic. As shown in Fig. 20, in the case of a pyramidally-shaped tip the indentation not only exhibits sharp edges, but also the region around the indentation, where polymer material is piled up, is anisotropic. The pile-up characteristics will be discussed in detail below. At this point we take it as an indication of the relevance of the heat transfer on the measurements.

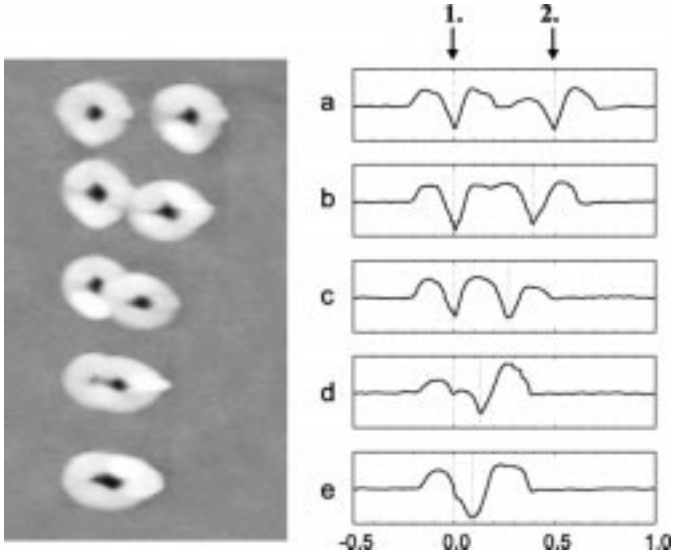

Fig. 24. Indentations in a PMMA film at several distances. The depth of the indentations is ~15 nm, about the thickness of the PMMA layer. The indentations on the left-hand side were written first, then a second series of indentations were made with decreasing distance to the first series in going from a to e.

One of the most striking conclusions of our model of the bit-writing process is that it should in principle work for most polymer materials. The general behavior of the mechanical properties as a function of temperature and frequency is similar for all polymers [30]. The glass-transition temperature T_g would then be one of the main parameters determining the threshold writing temperature.

A verification of this was found experimentally by comparing various polymer films. The samples were prepared in the same way as the PMMA samples discussed earlier [19]: by spin casting thin films (10–30 nm) onto a silicon wafer with a photo-resist buffer. Then threshold measurements were done by applying heat pulses with increasing current (or temperature) to the tip while the load and the heating time were held constant (load about 10 nN and heating time 10 μs). Examples of such measurements are shown in Fig. 21, where the increasing size and depth of bits can seen for different heater temperatures. A threshold can be defined based on such data and compared

with the glass-transition temperature of these materials. The results show a clear correlation between the threshold heater temperature and the glass-transition temperature (see Fig. 22).

It is worth looking at the detailed shapes of the written bits. The polymer material around an indentation appears piled-up as can be seen, for example, in Fig. 20. This is not only material that was pushed aside during indentation formation as a result of volume conservation. Rather, the flash heating by the tip and subsequent rapid cooling result in an increase of the specific volume of the polymer. This phenomenon that the specific volume of a polymer can be increased by rapidly cooling a sample through the glass transition [30] is well-known. Our system allows a cooling time of the order of microseconds, which is much faster than the fastest rates that can be achieved with standard polymer-analysis tools. However, a quantitative measurement of the specific volume change cannot be easily done in our type of experiments. On the other hand, the pile-up effect serves as a convenient threshold thermometer. The outer perimeter of the donuts surrounding the indentations corresponds to the T_g isotherm, and the temperature in the enclosed area has certainly reached values larger than T_g during the indentation process. Based on our visco-elastic model, one would, thus, conclude that previously written bits that overlap with the pile-up region of a subsequently written bit should be erased.

That this pile-up effect actually works against the formation of an indentation can clearly be seen in the line scans of a series of indentations taken in Polysulfone (Fig. 23). Here, the heating of the tip was accompanied by a rather high normal force. The force was high enough to leave a small plastic indentation even if the tip was too cold to modify the polymer [Fig. 23(a)]. Then, with increasing tip heating, the indentations initially fill up in the piled-up region [Fig. 23(b)] before they finally become deeper [Fig. 23(c)].

The pile-up phenomenon turns out to be particularly beneficial for data-storage applications. The following example demonstrates the effect. If we look at the sequence of images in Fig. 24 taken on a standard PMMA sample, we find that the piled-up regions can overlap each other without disturbing the indentation. If the piled-up region of an individual bit-writing event, however, extends over the indented area of a previously written bit, the depth of the corresponding indentation decreases markedly [Fig. 24(d)]. This can be used for erasing written bits. However, if the pitch between two successive bits is decreased even further, this erasing process will no longer work. Instead a broader indentation is formed [Fig. 24(d)]. Hence, to exclude mutual interference, the minimum pitch between successive bits must be larger than the radius of the piled-up area around an indentation.

In the example shown in Fig. 24 the temperature was chosen so high that the ring around the indentations was very large, whereas the depth of the bit was limited by the stop layer underneath the PMMA material. Clearly, here the temperature was too high to form small bits, the minimum pitch being around 250 nm. However, by carefully optimizing all parameters it is possible to achieve areal densities of up to 1 Tb/in^2 as demonstrated in Fig. 3(c).

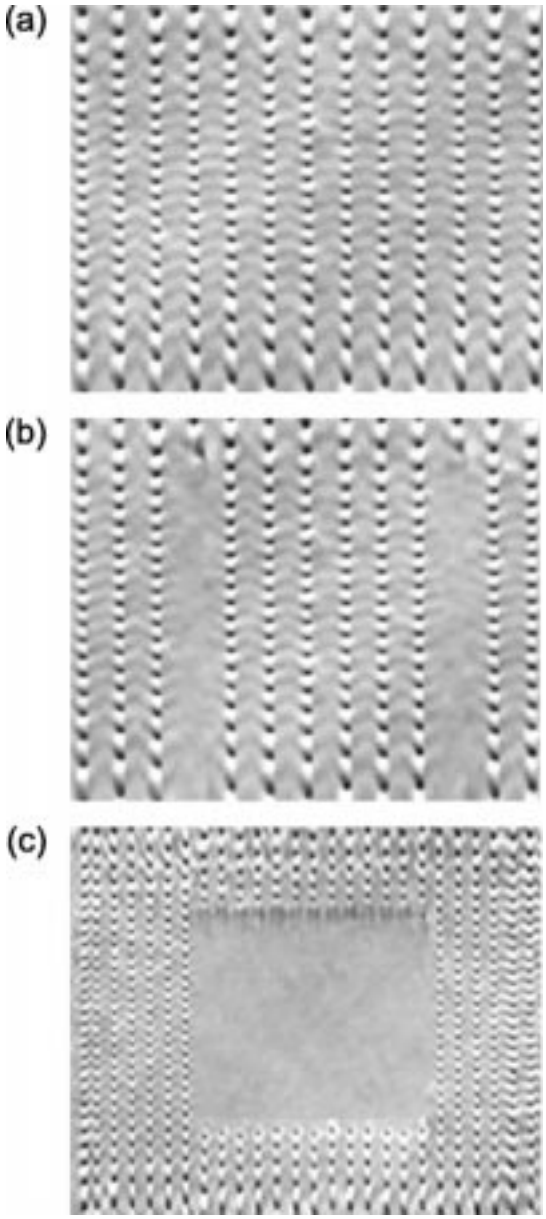

Fig. 25. Demonstration of the new erasing scheme. (a) Bit pattern with variable pitch in the vertical axis (fast scan axis) and constant pitch in the horizontal direction (slow scan axis) was prepared. (b) Then two of the lines were erased by decreasing the pitch in the vertical direction by a factor of three, showing that the erasing scheme works for individual lines. One can also erase entire fields of bits without destroying bits at the edges of the fields. This is demonstrated in (c), where a field has been erased from a bit field similar to the one shown in (a). The distance between the lines is 70 nm.

The new erasing scheme based on this volume effect switches from writing to erasing merely by decreasing the pitch of writing indentations. This can be done in a very controlled fashion as shown in Fig. 25, where individual lines or predefined subareas are erased. Hence, this new erasing scheme can be made to work in a way that is controlled on the scale of individual bits. Compared with earlier global erasing schemes [13], this simplifies erasing significantly.

With our simple visco-elastic model of bit writing we are able to formulate a set of requirements that potential candidate materials for millipede data storage have to fulfill. First, the material should ideally exhibit a well-defined glass-transition point

with a large drop of the shear modulus at T_g. Second, a rather high value of T_g on the order of 150 °C is preferred to facilitate thermal read-back of the data without destroying the information. We have investigated a number of materials to explore the T_g parameter space. The fact that all polymer types tested are suitable for writing small bits allows us to exercise the freedom of choice of polymer type to optimize in terms of the technical requirements for a device, such as lifetime of bits, polymer endurance of the read and write process, power consumption, etc. These are fields of ongoing research.

IX. Conclusion and Outlook

In conclusion, a very large 2-D array of local probes has been operated for the first time in a multiplexed/parallel fashion, and write/read storage operation in a thin polymer medium has been successfully demonstrated at densities of or significantly higher than those achieved with current magnetic storage systems. Densities and yield of operation achieved with this first demo are very encouraging, although considerable improvements are possible in both areas. Storage densities comparable to or even higher than 0.5–1 Tb/in^2 as demonstrated with single levers will be possible, whereas the high operating yield confirms the concept of global array approaching. Faster electronics will allow the levers to be operated at considerably higher rates.

The write/read data rate depends on the number of cantilevers operated in parallel, which consequently affects the overall power consumption. The high areal storage density and small form factor make millipede very attractive as a potential future storage technology in mobile applications, offering several gigabyte capacity and low power consumption at megabyte per second data rates.

Although we have demonstrated the first high-density storage operations with the largest 2-D AFM array chip ever built, there are a number of issues to be addressed before the millipede can be considered for commercial applications, just a few of which are mentioned here:

- overall system reliability, including bit stability, tip and medium wear, erasing/rewriting;
- limits of data rate (S/N ratio), areal density, array and cantilever size;
- CMOS integration;
- optimization of write/read multiplexing scheme;
- array-chip tracking;
- data rate versus power consumption tradeoffs.

A functional prototype storage system is currently being built in order to investigate these important aspects. The polymer medium is another important area of intense research. We have identified the fundamental physical mechanism of polymer deformation, which allows us to correlate polymer properties with millipede-relevant parameters, such as load and temperature dependence, for bit writing. Moreover, we have established a novel local erasing scheme based on our finding that indentations represent elastically stressed metastable states of the medium. The fact that bit writing is a robust process in terms of polymer selection opens up wide opportunities for medium optimization for complementary technical requirements. In addition to data storage in polymers or other media, and not excluding magnetics, we envision areas in nanoscale science and technology such as lithography, high-speed/large-scale imaging, molecular and atomic manipulation, and many others where millipede may open up new perspectives and opportunities.

Acknowledgment

The authors would like to give special thanks and appreciation to H. Rohrer for his contribution to the initial millipede vision and concept, and to their former collaborators, J. Brugger, now at the Swiss Federal Institute of Technology, Lausanne (Switzerland), M. I. Lutwyche, now at Seagate, Pittsburg, IL, and W. P. King, now at Stanford University, CA, as well as to K. Goodson, T. W. Kenny, and C. F. Quate of Stanford University.

The authors are also pleased to acknowledge the technical contributions of, stimulating discussions with, and encouraging support of their colleagues R. Beyeler, R. Germann, and P. F. Seidler of the IBM Zurich Research Laboratory, and J. Mamin, D. Rugar, and B. D. Terris of the IBM Almaden Research Center.

Special thanks go to J. Frommer, C. Hawker, B. van Horn, H. Ito, V. Lee, J. Mamin, and R. Miller of the IBM Almaden Research Center, J. D. Gelorme and J. M. Shaw of the IBM T. J. Watson Research Center, Yorktown Heights, NY, as well as G. Hefferon and W. Moreau of IBM East Fishkill for their enthusiastic support in identifying and synthesizing alternative polymer media materials, which provide the basis for systematic media investigation.

In addition, it is the authors' pleasure to acknowledge their colleagues T. Albrecht, T. Antonakopoulos, P. Bächtold, G. Cherubini, A. Dholakia, E. Eleftheriou, T. Loeliger, H. Pozidis, A. Sharma, and S. Sri-Jayantha for their invaluable contributions to their storage-system prototyping effort.

References

[1] E. Grochowski and R. F. Hoyt, "Future trends in hard disk drives," *IEEE Trans. Magn.*, pt. 2, vol. 32, pp. 1850–1854, May, 1996.

[2] H. J. Mamin and D. Rugar, "Thermomechanical writing with an atomic force microscope tip," *Appl. Phys. Lett.*, vol. 61, pp. 1003–1005, 1992.

[3] R. P. Ried, H. J. Mamin, B. D. Terris, L. S. Fan, and D. Rugar, "6-MHz 2-N/m piezoresistive atomic-force-microscope cantilevers with incisive tips," *J. Microelectromech. Syst.*, vol. 6, pp. 294–302, 1997.

[4] B. D. Terris, S. A. Rishton, H. J. Mamin, R. P. Ried, and D. Rugar, "Atomic force microscope-based data storage: Track servo and wear study," *Appl. Phys. A*, vol. 66, pp. S809–S813, 1998.

[5] H. J. Mamin, B. D. Terris, L. S. Fan, S. Hoen, R. C. Barrett, and D. Rugar, "High-density data storage using proximal probe techniques," *IBM J. Res. Develop.*, vol. 39, pp. 681–700, 1995.

[6] H. J. Mamin, R. P. Ried, B. D. Terris, and D. Rugar, "High-density data storage based on the atomic force microscope," *Proc. IEEE*, vol. 87, pp. 1014–1027, 1999.

[7] D. A. Thompson and J. S. Best, "The future of magnetic data storage technology," *IBM J. Res. Develop.*, vol. 44, pp. 311–322, May 2000.

[8] G. K. Binnig, H. Rohrer, and P. Vettiger, "Mass-storage applications of local probe arrays," U.S. Patent 5 835 477, Nov. 10, 1998.

[9] P. Vettiger, J. Brugger, M. Despont, U. Drechsler, U. Dürig, W. Häberle, M. Lutwyche, H. Rothuizen, R. Stutz, R. Widmer, and G. Binnig, "Ultrahigh density, high-data-rate NEMS-based AFM data storage system," *J. Microelectron. Eng.*, vol. 46, pp. 11–17, 1999.

[10] M. Lutwyche, C. Andreoli, G. Binnig, J. Brugger, U. Drechsler, W. Häberle, H. Rohrer, H. Rothuizen, and P. Vettiger, "Microfabrication and parallel operation of 5 × 5 2D AFM cantilever array for data storage and imaging," in *Proc. IEEE 11th Int. Workshop MEMS*, 1998, pp. 8–11.

[11] B. W. Chui, H. J. Mamin, B. D. Terris, D. Rugar, K. E. Goodson, and T. W. Kenny, "Micromachined heaters with 1-μs thermal time constants for AFM thermomechanical data storage," in *Proc. IEEE Transducers*, 1997, pp. 1085–1088.
[12] W. P. King, J. G. Santiago, T. W. Kenny, and K. E. Goodson, "Modeling and prediction of sub-micrometer heat transfer during thermomechanical data storage," in *Proc. ASME MEMS*, vol. 1, 1999, pp. 583–588.
[13] G. Binnig, M. Despont, U. Drechsler, W. Häberle, M. Lutwyche, P. Vettiger, H. J. Mamin, B. W. Chui, and T. W. Kenny, "Ultra high-density AFM data storage with erase capability," *Appl. Phys. Lett.*, vol. 74, pp. 1329–1331, 1999.
[14] G. K. Binnig, M. Despont, W. Häberle, and P. Vettiger, "Method of forming ultrasmall structures and apparatus therefor," Filed at the U.S. Patent Office, Application no. 147 865, Mar. 17, 1999.
[15] G. K. Binnig, J. Brugger, W. Häberle, and P. Vettiger, "Investigation and/or manipulation device," Filed at the U.S. Patent Office, Application no. 147 867, Mar. 17, 1999.
[16] S. M. Sze, *Physics of Semiconductors Devices*. New York: Wiley, 1981.
[17] T. S. Ravi and R. B. Marcus, "Oxidation sharpening of silicon tips," *J. Vac. Sci. Technol. B*, vol. 9, pp. 2733–2737, 1991.
[18] M. Despont, J. Brugger, U. Drechsler, U. Dürig, W. Häberle, M. Lutwyche, H. Rothuizen, R. Stutz, R. Widmer, G. Binnig, H. Rohrer, and P. Vettiger, "VLSI-NEMS chip for AFM data storage," in *Proc. Tech. Dig. 12th IEEE Int. Micro Electro Mechanical Systems Conf. MEMS*, 1999, pp. 564–569.
[19] P. Vettiger, M. Despont, U. Drechsler, U. Dürig, W. Häberle, M. I. Lutwyche, H. E. Rothuizen, R. Stutz, R. Widmer, and G. K. Binnig, "The 'millipede'—more than one thousand tips for future AFM data storage," *IBM J. Res. Develop.*, vol. 44, pp. 323–340, May 2000.
[20] S. C. Minne, G. Yaralioglu, S. R. Manalis, J. D. Adams, A. Atalar, and C. F. Quate, "Automated parallel high-speed atomic force microscopy," *Appl. Phys. Lett.*, vol. 72, pp. 2340–2342, 1998.
[21] M. Lutwyche, U. Drechsler, W. Häberle, R. Widmer, H. Rothuizen, P. Vettiger, and J. Thaysen, "Planar micro-magnetic $x/y/z$ scanner with five degrees of freedom," in *Magnetic Materials, Processes, and Devices: Applications to Storage and Micomechanical Systems (MEMS)*, L. Romankiw, S. Krongelb, and C. H. Ahn, Eds. Pennington, NJ: The Electrochemical Society, 1999, vol. 98-20, pp. 423–433.
[22] H. Rothuizen, U. Drechsler, G. Genolet, W. Häberle, M. Lutwyche, R. Stutz, R. Widmer, and P. Vettiger, "Fabrication of a micromachined magnetic $X/Y/Z$ scanner for parallel scanning probe applications," *Microelectron. Eng.*, vol. 53, pp. 509–512, 2000.
[23] J.-J. Choi, H. Park, K. Y. Kim, and J. U. Jeon, "Electromagnetic micro x–y stage for probe-based data storage," *J. Semicond. Technol. Sci.*, vol. 1, pp. 84–93, 2001.
[24] H. Lorenz, M. Despont, N. Fahrni, J. Brugger, P. Vettiger, and P. Renaud, "High-aspect-ratio, ultrathick, negative-tone near-UV photoresist and its applications for MEMS," *Sens. Actuators B, Chem.*, vol. 64, pp. 33–39, 1998.
[25] "Sylgard 184 silicon elastomer," Dow Corning, Midland, MI.
[26] H. Rothuizen, M. Despont, U. Drechsler, G. Genolet, W. Häberle, M. Lutwyche, R. Stutz, and P. Vettiger, "Compact copper/epoxy-based micromachined electromagnetic scanner for scanning probe applications," in Proc. IEEE 15th Int. Conf. Micro Electro Mechanical Systems MEMS, Las Vegas, NV, 2002, to be published.
[27] C. Q. Davis and D. Freeman, "Using a light microscope to measure motions with nanometer accuracy," *Opt. Eng.*, vol. 37, pp. 1299–1304, 1998.
[28] M. I. Lutwyche, M. Despont, U. Drechsler, U. Dürig, W. Häberle, H. Rothuizen, R. Stutz, R. Widmer, G. K. Binnig, and P. Vettiger, "Highly parallel data storage system based on scanning probe arrays," *Appl. Phys. Lett.*, vol. 77, pp. 3299–3301, 2000.
[29] K. Fuchs, Chr. Friedrich, and J. Weese, "Viscoelastic properties of narrow-distribution poly(methyl metacrylates)," *Macromolecules*, vol. 29, pp. 5893–5901, 1996.
[30] J. D. Ferry, *Viscoelastic Properties of Polymers*, 3rd ed. New York: Wiley, 1980.
[31] M. Lutwyche, C. Andreoli, G. Binnig, J. Brugger, U. Drechsler, W. Häberle, H. Rohrer, H. Rothuizen, P. Vettiger, G. Yaralioglu, and C. Quate, "5 × 5 2D AFM cantilever arrays: A first step toward a terabit storage device," *Sens. Actuators A, Phys.*, vol. 73, pp. 89–94, 1999.
[32] W. P. King, T. W. Kenny, K. E. Goodson, G. L. W. Cross, M. Despont, U. Dürig, H. Rothuizen, G. Binnig, and P. Vettiger, "Design of atomic force microscope cantilevers for combined thermomechanical writing and thermal reading in array operation," J. Microelectromech. Sys., submitted for publication.
[33] M. Despont, J. Brugger, U. Drechsler, U. Dürig, W. Häberle, M. Lutwyche, H. Rothuizen, R. Stutz, R. Widmer, G. Binnig, H. Rohrer, and P. Vettiger, "VLSI-NEMS chip for parallel AFM data storage," *Sens. Actuators A, Phys.*, vol. 80, pp. 100–107, 2000.

P. Vettiger (A'77–M'77–SM'95–F'01) received the degree in communications technology and electronics engineering from Zurich Technical State University, Zurich, Switzerland, in 1965.

Since 1967, he has worked as a Research Staff Member and Project Manager at the IBM Research, Zurich Research Laboratory, Rüschlikon, Switzerland. In 1979, he initiated and established nanoscale fabrication techniques based on electron-beam lithography for superconducting, electronic, and opto-electronic devices and circuits. Later, he became Head of the micro- and nanofabrication activities in the laboratory's Technology Department. He spent extended time at the IBM T. J. Watson Research Center, Yorktown Heights, NY, and at IBM's Semiconductor Plant, East Fishkill, NY. Since 1995, he has been Manager of the Micro/Nanomechanics Group within the Science and Technology Department. His current interests and research activities are focused on micro/nanomechanical devices and systems for scanning probe data storage including aspects of fabrication and electronics integration for future VLSI N(M)EMS.

Mr. Vettiger holds several IBM outstanding and invention achievement awards. He is a member of the IBM Technical Academy, and more recently was honored with a Doctor *honoris causa* from the University of Basel, Basel, Switzerland.

G. Cross received the B.Sc. degree in physics from the University of Victoria, BC, Canada, in 1991 and the M.Sc. and Ph.D. degrees from McGill University, Montreal, QC, Canada, in 1995 and 1999, respectively.

From 1999 to 2001, he completed a postdoctorate in the Micro/Nanomechanics group at IBM Research, Zurich Research Laboratory, Rüschlikon, Switzerland, where he worked on thermomechanical transducer characterization and polymer storage media studies. Currently, he is a Postdoctoral Fellow at the University of Zurich, Zurich, Switzerland, studying electron point source applications for nanotechnology.

M. Despont received the degree in microtechnology from the Swiss Federal Institute of Technology, Lausanne, Switzerland, in 1993 and the Ph.D. degree in physics from the Institute of Microtechnology, University of Neuchâtel, Neuchâtel, Switzerland, in 1996, with a dissertation on the microfabrication of miniaturized electron lenses.

In 1996, he was a Postdoctoral Fellow at IBM Research, Zurich Research Laboratory, Rüschlikon, Switzerland, where he worked on the development of various cantilever-based sensors. He then spent one year as a Visiting Scientist at the Seiko Instrument Research Laboratory, Japan. Since returning to the IBM Zurich Research Laboratory, his current research has been focused on the development of micro- and nanomechanical devices.

U. Drechsler joined the IBM Plant, Sindelfingen, Germany, in 1983, starting with a three-year course of study in chemistry. Afterwards, she worked in the fabrication line for multilayer ceramic packaging, where she was promoted to Section Head, in 1993. In 1996, she joined the Micro/Nanomechanics group, IBM Research, Zurich Research Laboratory, Rüschlikon, Switzerland, working on silicon micromachining and processing techniques for millipede array chips and processing-related work for other department projects. Currently, she is a Processing Engineer in the Science and Technology Department, IBM Research, where she is responsible for the organization and operation of the department cleanroom.

U. Dürig received the degree in experimental physics and the Ph.D. degree, both from the Swiss Federal Institute of Technology, Zurich, Switzerland, in 1979 and 1984, respectively.

He was then a Postdoctoral Fellow at the IBM Zurich Research Laboratory, Rüschlikon, Switzerland, working on near-field optical microscopy in D. Pohl's group. In 1986, he became a Research Staff Member and worked in the field of scanning tunneling and force microscopy, investigating metallic adhesion, growth morphology of magnetic thin films, and surface melting. In 1997, he joined the Micro/Nanomechanics group working on characterizing tip polymer interactions.

B. Gotsmann received the Ph.D. degree from the University of Münster, Münster, Germany, in 2000, with a dissertation on dynamic force microscopy.

Since 2001, he had been a Postdoctoral Fellow at the Micro/Nanomechanics group of the IBM Research, Zurich Research Laboratory, Rüschlikon, Switzerland, working on the characterization of polymer media and the thermomechanical read and write process.

W. Häberle joined the IBM Semiconductor Plant, Sindelfingen, Germany, in 1974, for his education in physics. Afterwards, he was promoted to Group Leader in the Quality Control Department of the semiconductor line. In 1987, he joined the IBM Physics Group of Prof. G. K. Binnig at the University of Munich, Munich, Germany, where he contributed to the development of AFMs for applications to liquids for investigating living cells. In 1995, he transferred to the IBM Research, Zurich Research Laboratory, Rüschlikon, Switzerland, where he was responsible for prototyping a new low-cost AFM instrument with good price/performance, which has since been commercialized by Seiko Instruments, Japan. Currently, he is a Development Engineer in the Science and Technology Department at IBM Research. He has been involved in various aspects of millipede, including writing/reading experiments with the first 32 × 32 array chip, lifetime stability tests of the polymer and the levers, and a new nanomechanical scan device (nanoscanner) for the prototype of the millipede storage device.

M. A. Lantz received the B.Sc. and M.Sc. degrees in electrical engineering from the University of Alberta, Edmonton, AB, Canada, in 1991 and 1993, respectively, and the Ph.D. degree from the University of Cambridge, Cambridge, U.K., in 1997, for work in the field of scanning probe microscopy.

From 1997 to 1999, he was a Postdoctoral Researcher at the Joint Research Center for Atom Technology, National Institute for Advanced Interdisciplinary Research, Ibaraki, Japan, investigating the application of scanning probes in biophysics. From 1999 to 2001, he conducted research in the area of low-temperature scanning force microscopy at the University of Basel, Basel, Switzerland. In 2001, he became a Research Staff Member with the Micro/Nanomechanics group, IBM Research, Zurich Research Laboratory, Rüschlikon, Switzerland. His current research activities are focused on micro- and nanomechanical devices and systems for scanning-probe-based data storage.

H. E. Rothuizen received the Ph.D. degree in applied physics from the Swiss Federal Institute of Technology, Lausanne, Switzerland, in 1994, for work on selective area epitaxial growth of III–V semiconductor materials.

In 1996, he became a Research Staff Member at the IBM Research, Zurich Research Laboratory, Rüschlikon, Switzerland, and since then he has worked on the fabrication of various ultrasmall structures using electron-beam lithography. He is currently involved in the development of micromechanical sensors and actuators for data storage applications.

R. Stutz was responsible for the fabrication technological aspect of holography and integrated and microoptical systems on the technical staff of the Paul Scherrer Institute (PSI), and the Centre Suisse d'Electronique et de Microtechnique (CSEM), Zurich, Switzerland. In 1998, he joined the Micro/Nanomechanics Group, IBM Research, Zurich Research Laboratory, Rüschlikon, Switzerland, where he is currently a Senior Technical Specialist. His current technical responsibilities and interests include electro-plating, plasma sputter deposition, surface modification by stamping techniques and focused ion beam (FIB) machining for micromechanical devices.

G. K. Binnig received the Ph.D. degree from the University of Frankfurt, Frankfurt, Germany, in 1978, with a dissertation on superconductivity.

Since 1978, he has been a Research Staff Member at IBM Research, Zurich Research Laboratory, Rüschlikon, Switzerland. From 1985 to 1986, he was on sabbatical at the IBM Almaden Research Center, San Jose, CA. From 1985 to 1988, he was a Guest Professor at Stanford University, Stanford, CT. From 1987 to 1995, he headed the IBM Physics Group at the University of Munich, Munich, Germany, where he received an honorary professorship in 1987. His main fields of activity during that time were scanning tunneling microscopy and atomic force microscopy. His current fields of research include micro- and nanosystem techniques and the theory of "Fractal Darwinism," which he developed to describe complex systems.

Dr. Binnig has received numerous awards including the Nobel Prize in Physics for the development of the scanning tunneling microscope, which he invented together with Heinrich Rohrer, in 1986.